A RAO-BLACKWELLIZED PARTICLE FILTER FOR JOINT PARAMETER ESTIMATION AND BIOMASS TRACKING IN A STOCHASTIC PREDATOR-PREY SYSTEM

Laura Martín-Fernández

Departamento de Física Aplicada, Universidad de Granada
Avda. Fuentenueva s/n, 18071 Granada, Spain

Gianni Gilioli

Dipartimento di Scienze Biomediche e Biotecnologie, Università di Brescia
Viale Europa 11, 25125 Brescia, Italy

Ettore Lanzarone

CNR-IMATI
Via Bassini 15, 20133 Milano, Italy

Joaquín Míguez

Departamento de Teoría de la Señal y Comunicaciones, Universidad Carlos III de Madrid
Avda. de la Universidad 30, 28911 Leganés, Madrid, Spain

Sara Pasquali and Fabrizio Ruggeri

CNR-IMATI
Via Bassini 15, 20133 Milano, Italy

Diego P. Ruiz

Departamento de Física Aplicada, Universidad de Granada
Avda. Fuentenueva s/n, 18071 Granada, Spain

(Communicated by the associate editor Susanne Ditlevsen)

ABSTRACT. Functional response estimation and population tracking in predator-prey systems are critical problems in ecology. In this paper we consider a stochastic predator-prey system with a Lotka-Volterra functional response and propose a particle filtering method for: (a) estimating the behavioral parameter representing the rate of effective search per predator in the functional response and (b) forecasting the population biomass using field data. In particular, the proposed technique combines a sequential Monte Carlo sampling scheme for tracking the time-varying biomass with the analytical integration of the unknown behavioral parameter. In order to assess the performance of the method, we show results for both synthetic and observed data collected in an acarine predator-prey system, namely the pest mite *Tetranychus urticae* and the predatory mite *Phytoseiulus persimilis*.

---

1. **Introduction.** Biological control strategies are based on the release of agents to control plant pest. These strategies are difficult to establish with scientific rigor because essential, but not always available, twofold information is required: the current abundance of pest population and properties of the predator functional response, i.e., the *per capita* rate of predation. Furthermore, the decision on time and amount of predator released has to be taken into the dynamical framework of predator-prey interaction.

This complexity suggests that definition and evaluation of biological control strategies may be done by modelling tools. Such tools can predict population abundance and damage level, as well as efficacy and time required by the predator for prey control. Two major components characterize predator-prey dynamics, the numerical response (i.e., prey growth) and the functional response. The first component can be easily estimated starting from biological data at individual level made available by the classical experimental approach based on the analysis of the life-history strategies. Experimental approaches have also been used for the estimation of the functional form and parameters of the predator functional response. However, it has been recognized that experimental approaches encounter important limitations due to the artificial experimental set-up conditioning the performances of the predator [44]. To overcome these limitations methodologies for functional response estimation based on time-series data from field survey have been proposed [29, 23].

Gilioli *et al.* [23, 24] presented a methodology which offers the advantage of obtaining parameter estimation in linear and non-linear functional responses from field data with limited assumptions on the properties of the predator-prey dynamics (e.g., the zero abundance data can not be used). However, the method requires the consideration of an entire dataset of populations dynamics and can be applied only at the end of the interaction between the populations, or after a certain time including, at least, an entire cycle of predator-prey interaction. This represents an important limitation in the practical implementation of modelling tools for decision support in the design of strategies of predator release.

The availability of methods for the estimation of parameters in functional response models during predator-prey interaction allows to continuously improve their reliability, to the extent that available information may greatly improve the possibility to use predator-prey models for decision support in biological control. These methods are suitable for the adaptive management framework, i.e., a systematic, cyclic process for continually improving management policies and practices (tactics, strategies) based on lessons learnt from operational activities [13, 41, 23]. Furthermore, the advantage of the adaptive approach is not only the improvement of the estimate according to the level of information, but also the possibility of an easy adaptation of the estimation procedure to the specific case of concern (e.g., differences in host plant species, in plants spatial arrangement, and in environmental conditions).

In this paper we propose a method to deal with the problem of inferring feeding rate indirectly from sampling population dynamics data. The parameter of the functional response is estimated during the establishment and the time evolution of population interactions. The proposed methodology is based on the description of the population dynamics through a stochastic predator-prey model of Lotka-Volterra type, coupled with a functional response parameter estimation based on a set of field data, as suggested in [23]. The choice of the Lotka-Volterra model is

justified by the advantage offered by its conditionally-linear structure, which allows the application of an efficient parameter estimation method.

The estimation problem herein addressed can be considered as part of the class of parameter estimation problems in discretely observed diffusion processes, which is a topic widely discussed in the literature [37, 20, 1, 6, 43, 39, 42]. In recent years, this problem has been tackled in the case of few available observations considering the introduction of latent data [21, 22, 26, 23, 24]. In particular, Bayesian approaches based on MCMC algorithms have been presented in [23, 24] to deal with stochastic population dynamics using a small set of field data. The key ingredient of the approach proposed in this paper is a sequential Monte Carlo (SMC) method [33, 16, 15], or particle filters (PFs), a technique that has been less commonly used in ecology compared to MCMC algorithms. PFs are recursive Monte Carlo algorithms for the approximation of the sequence of posterior probability distributions of the variables (and, sometimes, the parameters) of interest in state-space random dynamic models. The initial application of PFs in ecology has been related to the prediction of ecosystem state variables [17], while more recent works advocate the use of PFs to jointly estimate the time-varying state variables and the static behavioral parameters. For estimating the latter parameters, a PF based on augmenting the system state with the static parameters is proposed in [19], while in [18] an iterative state-augmented particle filter is used to jointly estimate the motion parameters and the state. Knape and De Valpine [31] propose an MCMC algorithm combined with sequential Monte Carlo techniques (PFMCMC) that explores the hidden states using PFs, while the process and observation parameters are estimated using an MCMC algorithm. The recently proposed particle MCMC (PMCMC) methodology [3] has been applied to a related problem (the estimation of the constant reaction rates in a stochastic kinetic model) in [27]. PMCMC is a computationally intensive MCMC-type of algorithm that uses PFs as auxiliary tools to build up the proposal kernels.

In all these works [17, 19, 18, 31], the problem of estimating the (static) parameters in the dynamic model is addressed by Monte Carlo sampling, i.e., they are handled in the same manner as the (time varying) state variables. However, it is known from the particle filtering literature (see, e.g., [4, 8]) that this approach has serious limitations and, at its best, it introduces additional Monte Carlo variance in the estimates computed using the empirical distributions produced by the PF. In this paper, we adopt the stochastic predator-prey model studied in [23] and show how a PF can be designed for the joint estimation of the dynamical population biomass and the feeding rate, an unknown parameter which determines the functional response of the predator to prey abundance. The key feature of the proposed method is that Monte Carlo sampling is only necessary on the space of the dynamic variables (the prey and predator biomass) while the functional-response parameter is handled analytically. This holds because of the conditionally linear structure of the Lotka-Volterra model[1], and the resulting algorithm is an example of Rao-Blackwellization in particle filtering (see, e.g., [16, 8], also known as mixture Kalman filtering [11]). Compared to standard PFs, this approach reduces the variance of the estimators.

We have applied the proposed technique on both synthetic and field data relative to an acarine predator-prey system relevant to biological control, the pest mite

---

[1]The model is linear on the feeding rate parameter conditional on the population biomass.

Tetranychus urticae and the predator mite *Phytoseiulus persimilis*. Numerical results show an improved accuracy in the biomass tracking compared to the MCMC algorithm applied in [23] over the same field dataset.

The rest of the paper is organized as follows. In Section 2 we describe the stochastic predator-prey model of interest and rewrite it as a state-space model. The Rao-Blackwellized PF for joint biomass tracking and parameter estimation is introduced in Section 3. In Section 4 we apply the proposed method to synthetic data and field data and carry out the comparison with the method of [23]. Finally, a summary and some conclusions are presented in Section 5.

2. Dynamic model.

2.1. Lotka-Volterra stochastic dynamic model.
We investigate a stochastic Lotka-Volterra type of model for the dynamics of a prey population and a predator population at continuous time t. The model adopts a logistic form for the growth of the prey, so as to take into account intra-specific competition. It is based on [23] and it can be described as

$$\begin{cases} dx_t & = [rx_t(1 - x_t) - q_0 x_t y_t]dt - \sigma x_t y_t dw_t^{(1)} + \varepsilon x_t dw_t^{(2)}, \\ dy_t & = [cq_0 x_t y_t - uy_t]dt + c\sigma x_t y_t dw_t^{(1)} + \eta y_t dw_t^{(3)}, \end{cases} \quad (1)$$

where

- x_t and y_t are the biomass of prey and predator, respectively, at time t per habitat unit normalized with respect to the prey carrying capacity per habitat unit (plant);
- r is the specific growth rate of the prey;
- c is the maximum production rate of the predator;
- u is the specific loss rate of the predator due to natural mortality;
- q_0 is a positive constant representing the efficiency of the predation process [7].

We consider random errors due to demographic stochasticity [10, 36] (modeled by the noise process $w_t^{(1)}$) and environmental stochasticity [36] (modeled by the noise processes $w_t^{(2)}$ and $w_t^{(3)}$). Moreover, we assume that $w_t^{(1)}$, $w_t^{(2)}$ and $w_t^{(3)}$ are independent Wiener processes, whereas the parameters σ, ε and η have been estimated by a least-squares method in [23] using an experimental dataset different from the field data studied in Section 4.2.

The lumped parameters r, c, u are species-specific and have been estimated in [7]. Thus, the behavioral parameter q_0 in the functional response $q_0 x_t y_t$ is the only unknown variable and has to be estimated. This is exactly the same problem addressed in [23]. The values used for $\sigma, \varepsilon, \eta, r, c$ and u are given explicitly in Section 4.

In order to apply the particle filtering methodology, we discretize Eq. (1) using the Euler scheme and obtaining the following stochastic discrete-time model

$$\begin{aligned} x_{k+1} & = x_k + \tau_k \left[rx_k(1 - x_k) - q_0 x_k y_k \right] - \sigma x_k y_t \Delta w_{k+1}^{(1)} + \varepsilon x_k \Delta w_{k+1}^{(2)}, \\ y_{k+1} & = y_k + \tau_k \left[cq_0 x_k y_k - uy_k \right] + c\sigma x_k y_k \Delta w_{k+1}^{(1)} + \eta y_k \Delta w_{k+1}^{(3)}, \end{aligned} \quad (2)$$

where $k = 0, 1, ..., S$ denotes the discrete time instants, S the final time instant of the studied time period, and τ_k is the time step used in the Euler approximation. The increments of the Wiener processes, $\Delta w_{k+1}^{(1)}$, $\Delta w_{k+1}^{(2)}$ and $\Delta w_{k+1}^{(3)}$ (where $\Delta w_{k+1}^{(i)} =$

$w^{(i)}((k+1)\tau_k) - w^{(i)}(k\tau_k)$, $i = 1, 2, 3$), are independent Gaussian variables with zero mean and variance τ_k.

Next, we define a state-space model with the unknown parameter q_0 as the single state "variable" (Section 2.2) and we extend this state-space model to put it into a format adequate to track the biomass variables x_{k+1} and y_{k+1}, with q_0 still unknown (Section 2.3).

2.2. **State-space Markov model.** Without loss of generality, in the sequel we assume $\tau_k = \tau$ for any k for the sake of clarity in the notation. We define the biomass increments $\Delta x_{k+1} = x_{k+1} - x_k$ and $\Delta y_{k+1} = y_{k+1} - y_k$, where $k = 0, ..., S-1$. Hence, the dynamic model of Eq. (2) can be rewritten as

$$\begin{aligned}
\Delta x_{k+1} &= \tau r x_k (1 - x_k) - \tau x_k y_k q_0 - \sigma x_k y_k \Delta w_{k+1}^{(1)} + \varepsilon x_k \Delta w_{k+1}^{(2)}, \\
\Delta y_{k+1} &= -\tau u y_k + \tau c x_k y_k q_0 + c\sigma x_k y_k \Delta w_{k+1}^{(1)} + \eta y_k \Delta w_{k+1}^{(3)},
\end{aligned} \tag{3}$$

or, in a vectorial compact form,

$$\boldsymbol{\Delta}_{k+1} = \mathbf{h}_{k+1} + \mathbf{g}_{k+1} q_0 + \mathbf{Q}_{k+1} \mathbf{w}_{k+1} \tag{4}$$

where

$$\boldsymbol{\Delta}_{k+1} = \begin{bmatrix} \Delta x_{k+1} \\ \Delta y_{k+1} \end{bmatrix}, \qquad \mathbf{w}_{k+1} = \begin{bmatrix} \Delta w_{k+1}^{(1)} \\ \Delta w_{k+1}^{(2)} \\ \Delta w_{k+1}^{(3)} \end{bmatrix},$$

$$\mathbf{h}_{k+1} = \begin{bmatrix} \tau r x_k (1 - x_k) \\ -\tau u y_k \end{bmatrix}, \qquad \mathbf{g}_{k+1} = \begin{bmatrix} -\tau x_k y_k \\ \tau c x_k y_k \end{bmatrix}, \text{ and} \tag{5}$$

$$\mathbf{Q}_{k+1} = \begin{bmatrix} -\sigma x_k y_k & \varepsilon x_k & 0 \\ c\sigma x_k y_k & 0 & \eta y_k \end{bmatrix}.$$

The model in Eq. (4) is nonlinear in the biomass variables x_k and y_k, but it is conditionally linear in q_0 (given the sequences $x_{0:k+1} = \{\mathbf{x}_0, \mathbf{x}_1, ..., \mathbf{x}_{k+1}\}$ and $y_{0:k+1} = \{\mathbf{x}_0, \mathbf{y}_1, ..., \mathbf{y}_{k+1}\}$). In this way, after defining $\mathbf{z}_{k+1} = \boldsymbol{\Delta}_{k+1} - \mathbf{h}_{k+1}$, we can rewrite Eq. (4) as a linear-Gaussian state-space model whose single state variable is the parameter of interest q_0 and $\mathbf{z}_{k+1}$ is the observation vector, namely

$$\begin{aligned}
q_{0,k+1} &= q_{0,k}, \\
\mathbf{z}_{k+1} &= \mathbf{g}_{k+1} q_{0,k+1} + \mathbf{Q}_{k+1} \mathbf{w}_{k+1}.
\end{aligned} \tag{6}$$

Eq. (6) defines q_0 as a static variable over time. The conditional density of $\mathbf{z}_{k+1}$ (or the likelihood of $q_{0,k+1}$) is Gaussian, namely[2]

$$p(\mathbf{z}_{k+1} | q_{0,k+1}) = \mathcal{N}(\mathbf{z}_{k+1}; \mathbf{g}_{k+1} q_{0,k+1}, \tau \mathbf{Q}_{k+1} \mathbf{Q}_{k+1}^\top). \tag{7}$$

where $\mathcal{N}(\boldsymbol{\alpha}; \boldsymbol{\mu}, \mathbf{C})$ denotes the multivariate Gaussian probability density function (pdf) of $\boldsymbol{\alpha}$ with mean vector $\boldsymbol{\mu}$ and covariance matrix $\mathbf{C}$.

Due to the linear structure in q_0 of the state-space model and the Gaussian likelihood, we can apply the Kalman filter [30, 2] to exactly compute the posterior distribution of q_0, denoted with $p(q_0 | \mathbf{z}_{1:S})$. Indeed, if we assume that q_0 is *a priori*

---

[2]We use p to denote probability functions, including densities and masses. The notation is argument-wise. For example, if x and y are continuous random variables, then $p(x)$ and $p(y)$ denote their probability density functions, possibly different. If x is a discrete random variable, then $p(x)$ denotes its probability mass function. Conditional densities and masses are indicated in the obvious way, e.g., $p(x|y)$. This notation is common in Bayesian analysis and in the particle filtering literature.

TABLE 1. Kalman filter for the computation of $p(q_0|\mathbf{z}_{1:k}) = \mathcal{N}(q_0; \hat{q}_{0,k}, P_k)$. The Kalman gain $\mathbf{s}_{k+1}$ is a 2×1 vector. The superscript $^\top$ denotes transposition.

Initialization. Let $p(q_0) = \mathcal{N}(q_0; \hat{q}_{0,0}, P_0)$.
Recursive step. For every $k \geq 0$:
1. Compute the Kalman gain: $\mathbf{s}_{k+1}^\top = P_k \mathbf{g}_{k+1}^\top (\mathbf{g}_{k+1} P_k \mathbf{g}_{k+1}^\top + \tau \mathbf{Q}_{k+1} \mathbf{Q}_{k+1}^\top)^{-1}$
2. Update the posterior mean: $\hat{q}_{0,k+1} = \hat{q}_{0,k} + \mathbf{s}_{k+1}^\top (\mathbf{z}_{k+1} - \mathbf{g}_{k+1} \hat{q}_{0,k})$
3. Update the posterior variance: $P_{k+1} = P_k - \mathbf{s}_{k+1}^\top \mathbf{g}_{k+1} P_k$

Gaussian, with mean $\hat{q}_{0,0}$ and variance P_0, i.e., $p(q_0) = \mathcal{N}(q_0; \hat{q}_{0,0}, P_0)$, then the posterior density at time k is also Gaussian,

$$p(q_0|\mathbf{z}_{1:k}) = \mathcal{N}(q_0; \hat{q}_{0,k}, P_k),$$

where $\hat{q}_{0,k} = \int q_0 \, p(q_0|\mathbf{z}_{1:k}) \, dq_0$ and $P_k = \int (q_0 - \hat{q}_{0,k})^2 \, p(q_0|\mathbf{z}_{1:k}) \, dq_0$ are the posterior mean and variance of the random parameter, respectively. The equations for the sequential computation $\hat{q}_{0,k}$ and P_k are given explicitly in Table 1 for completeness.

2.3. **Nonlinear gamma state-space model.** Assume that q_0 is known and the goal is the estimation of the biomass variables, x_{k+1} and y_{k+1}. It turns out convenient to consider the nonlinear state-space model, derived from Eq. (2)

$$\begin{aligned} \mathbf{b}_{k+1} &\sim p(\mathbf{b}_{k+1}|\mathbf{b}_k, q_0), \\ \mathbf{o}_{k+1} &\sim p(\mathbf{o}_{k+1}|\mathbf{b}_{k+1}), \end{aligned} \tag{8}$$

where $\mathbf{b}_{k+1} = \begin{bmatrix} x_{k+1} \\ y_{k+1} \end{bmatrix}$ is the state variable vector which collects the prey and predator biomass, $\mathbf{o}_{k+1} = \begin{bmatrix} o_{k+1}^x \\ o_{k+1}^y \end{bmatrix}$ is the vector of noisy biomass observations, $p(\mathbf{b}_{k+1}|\mathbf{b}_k, q_0)$ describes the conditional pdf of the state variables (in particular, we assume that the dynamics of x_k and y_k is defined as in Eq. (2)) and $p(\mathbf{o}_{k+1}|\mathbf{b}_{k+1})$ is the conditional density of the observations given the biomass of each population.

The state dynamics can be compactly expressed by the multivariate Gaussian pdf[3]

$$p(\mathbf{b}_{k+1}|\mathbf{b}_k, q_0) = \mathcal{N}(\mathbf{b}_{k+1}; \mathbf{b}_k + \mathbf{h}_{k+1} + \mathbf{g}_{k+1} q_0, \tau \mathbf{Q}_{k+1} \mathbf{Q}_{k+1}^\top) \tag{9}$$

where the mean depends on the behavioral parameter q_0, while $\mathbf{h}_{k+1}$, $\mathbf{g}_{k+1}$ and $\mathbf{Q}_{k+1}$ are quantities that depend on the biomasses at time k, as shown in Eq. (5).

We assume that the conditional density of the observations is gamma. In particular, if we denote with $\Gamma(\alpha; m, v)$ the gamma pdf of variable α, characterized by the mean m and the variance v, then

$$p(\mathbf{o}_{k+1}|\mathbf{b}_{k+1}) = \Gamma(o_{k+1}^x; x_{k+1}, d_x^2) \times \Gamma(o_{k+1}^y; y_{k+1}, d_y^2), \tag{10}$$

where the marginal variances, d_x^2 and d_y^2, have been fitted to the measurement-variance of experimental data (Section 4.2). We have modeled the conditional

---

[3]Let us remark that the density $p(\mathbf{b}_{k+1}|\mathbf{b}_k, q_0)$ only describes the dynamics of $\mathbf{b}_k$ when q_0 is available, otherwise the process $\mathbf{b}_k$ is not Markov. In particular, if q_0 is unknown, then $p(\mathbf{b}_{k+1}|\mathbf{b}_{0:k}) \neq p(\mathbf{b}_{k+1}|\mathbf{b}_k, q_0)$.

density of the observations as gamma to enforce that both o_{k+1}^x and o_{k+1}^y be non-negative, since the biomass of the species can not be negative in the real world. Other models, e.g., truncated Gaussian distributions, could have been adopted, but possibly at the expense of a higher computational complexity of the inference algorithms.

When q_0 is known, the model in Eq. (8) enables the derivation of standard particle filtering algorithms for tracking the biomass of each population, while, in combination with Eq. (6), it enables the derivation of efficient algorithms for joint parameter estimation and biomass tracking. The different possibilities are explored in Section 3.

3. **Computational inference.** We propose to apply a PF to approximate the sequence of posterior probability distributions of the population biomass given the observations, namely the distributions associated with the densities $p(\mathbf{b}_k|\mathbf{o}_{1:k})$, $k = 1, 2, ..., S$. If q_0 is known, this can be done running a standard particle filtering technique on the gamma state-space model of Section 2.3. When q_0 is unknown, we derive algorithms that only demand Monte Carlo sampling in the (2-dimensional) space of $\mathbf{b}_k$, while the behavioral parameter q_0 is integrated out analytically, both with complete and missing observations. The final aim is to improve the estimation of q_0 obtained in [23] while simultaneously tracking the biomass vector $\mathbf{b}_{k+1}$ with missing observations. In the rest of this Section we first introduce the notion of a stochastic filter and then proceed to derive practical implementations using the particle filtering methodology.

3.1. **Stochastic filtering.** Assume that the parameter $q_{0,k} = q_0$ is known for any k. From a Bayesian point of view, all the information required for inference on the biomass in $\mathbf{b}_k$ is given by the posterior distribution with density $p(\mathbf{b}_{k+1}|\mathbf{o}_{1:k+1}, q_0)$, where $\mathbf{o}_{1:k+1}$ is the sequence of observations collected up to time $k+1$. Using Bayes' theorem, the posterior pdf can be decomposed as

$$p(\mathbf{b}_{k+1}|\mathbf{o}_{1:k+1}, q_0) \propto p(\mathbf{o}_{k+1}|\mathbf{b}_{k+1})\, p(\mathbf{b}_{k+1}|\mathbf{o}_{1:k}, q_0), \qquad (11)$$

where the proportionality constant (i.e., $p(\mathbf{o}_{k+1}|\mathbf{o}_{1:k}, q_0)$), which is independent of $\mathbf{b}_{k+1}$, is omitted. The likelihood $p(\mathbf{o}_{k+1}|\mathbf{b}_{k+1})$ is given by the state-space model and

$$p(\mathbf{b}_{k+1}|\mathbf{o}_{1:k}, q_0) = \int p(\mathbf{b}_{k+1}|\mathbf{b}_k, q_0)\, p(\mathbf{b}_k|\mathbf{o}_{1:k}, q_0)\, d\mathbf{b}_k \qquad (12)$$

is the predictive pdf of the variables in $\mathbf{b}_{k+1}$ given the observations $\mathbf{o}_{1:k}$ and q_0.

The optimal stochastic filter is a device that combines Eqs. (11) and (12) to recursively compute the sequence of posterior pdf's $p(\mathbf{b}_{k+1}|\mathbf{o}_{1:k+1}, q_0)$ with $k = 0, 1, 2, ...$, starting from the prior density $p(\mathbf{b}_0)$. It is often written as a two-step procedure consisting in

(a) a prediction step, i.e., the computation of $p(\mathbf{b}_{k+1}|\mathbf{o}_{1:k}, q_0)$ via Eq. (12) ;
(b) an update step, i.e., the computation of $p(\mathbf{b}_{k+1}|\mathbf{o}_{1:k+1}, q_0)$ via Eq. (11).

In general, the stochastic filter does not admit an exact implementation, unless the state-space is discrete and finite or the model is linear and Gaussian [15]. In the latter case, $p(\mathbf{b}_{k+1}|\mathbf{o}_{1:k+1}, q_0)$ is Gaussian and it can be computed exactly at each time step $k = 0, 1, 2...$ using the algorithm known as Kalman filter [30] (see also, e.g., [2]).

If q_0 is unknown, the model is not Markov anymore, hence $p(\mathbf{b}_{k+1}|\mathbf{b}_k, \mathbf{o}_{1:k}) \neq p(\mathbf{b}_{k+1}|\mathbf{b}_k, q_0)$. As a consequence, the predictive step in the stochastic filter becomes

$$p(\mathbf{b}_{k+1}|\mathbf{o}_{1:k}) = \int p(\mathbf{b}_{k+1}|\mathbf{b}_k, \mathbf{o}_{1:k}) \, p(\mathbf{b}_k|\mathbf{o}_{1:k}) \, d\mathbf{b}_k.$$

Again, there is no closed form solution for this integral in general.

3.2. **Particle filtering.** Particle filters are methods for the approximate numerical implementation of the optimal stochastic filter. We first assume that q_0 is known in order to derive a standard sequential importance sampling (SIS) algorithm [16]. In particular, we apply importance sampling (see, e.g., [40]) to approximate the distribution with density $p(\mathbf{b}_{0:k+1}|\mathbf{o}_{1:k+1}, q_0)$. The latter pdf admits the recursive decomposition

$$p(\mathbf{b}_{0:k+1}|\mathbf{o}_{1:k+1}, q_0) \propto p(\mathbf{o}_{k+1}|\mathbf{b}_{k+1}) \, p(\mathbf{b}_{k+1}|\mathbf{b}_k, q_0) \, p(\mathbf{b}_{0:k}|\mathbf{o}_{1:k}, q_0), \qquad (13)$$

based on the Bayes' theorem, the Markov property of the sequence $\mathbf{b}_k$ and the conditional independence of the observations. If we draw M samples (often called particles) $\mathbf{b}_{0:k+1}^{(i)}$, $i = 1, ..., M$, from an importance function, or proposal pdf, which can be factorized as

$$q(\mathbf{b}_{0:k+1}) = q(\mathbf{b}_{k+1}|\mathbf{b}_{0:k}) \, q(\mathbf{b}_{0:k}) \qquad (14)$$

then an importance weight $v_{k+1}^{(i)}$ of the form

$$
\begin{aligned}
v_{k+1}^{(i)} &\propto \frac{p(\mathbf{o}_{k+1}|\mathbf{b}_{k+1}^{(i)}) \, p(\mathbf{b}_{k+1}^{(i)}|\mathbf{b}_k^{(i)}, q_0)}{q(\mathbf{b}_{k+1}^{(i)}|\mathbf{b}_{0:k}^{(i)})} \times \frac{p(\mathbf{b}_{0:k}^{(i)}|\mathbf{o}_{1:k}, q_0)}{q(\mathbf{b}_{0:k}^{(i)})} \\
&\propto \frac{p(\mathbf{o}_{k+1}|\mathbf{b}_{k+1}^{(i)}) \, p(\mathbf{b}_{k+1}^{(i)}|\mathbf{b}_k^{(i)}, q_0)}{q(\mathbf{b}_{k+1}^{(i)}|\mathbf{b}_{0:k}^{(i)})} v_k^{(i)}.
\end{aligned}
\qquad (15)
$$

is assigned to each sample $\mathbf{b}_{0:k+1}^{(i)}$. The weights are normalized (i.e., $\sum_{i=1}^{M} v_{k+1}^{(i)} = 1$) and this is the reason of the $\propto$ sign in Eq. (15).

From Eqs. (14) and (15), we observe that both the generation of samples and the computation of the weights can be done sequentially. For instance, if we choose the prior pdf $p(\mathbf{b}_{0:k+1}) = p(\mathbf{b}_{k+1}|\mathbf{b}_k, q_0) \prod_{n=1}^{k} p(\mathbf{b}_n|\mathbf{b}_{n-1}, q_0) \, p(\mathbf{b}_0)$ as an importance function, then the sample $\mathbf{b}_{k+1}^{(i)}$ can be drawn from $p(\mathbf{b}_{k+1}|\mathbf{b}_k^{(i)}, q_0)$ (independently of $\mathbf{b}_{0:k-1}^{(i)}$) and the corresponding weight reduces to

$$v_{k+1}^{(i)} \propto v_k^{(i)} p(\mathbf{o}_{k+1}|\mathbf{b}_{k+1}^{(i)}).$$

Table 2 summarizes the standard SIS algorithm with prior importance function for the gamma state-space model of Section 2.3. This is also the well-known *bootstrap* filter of [28], or a special (actually the simplest) case of the auxiliary PF in [38]. Note that the algorithm includes a resampling step that consists in drawing M times, with replacement, from the discrete probability distribution given by the particles and their weights. Intuitively, we are randomly selecting the most "promising" particles (those with large importance weights) to be propagated in the next recursive step, while (randomly) discarding those with low weights. This algorithmic step is necessary to avoid the degeneracy of the importance weights over time [16]. Although several forms of resampling can be applied [9, 14, 5], we adopt the conceptually simple multinomial resampling method. Even if it is not indispensable to perform resampling at every time step and it can be done periodically or according to some measure of weight degeneracy [16, 14], here we assume resampling is

TABLE 2. Standard SIS algorithm with multinomial resampling (SISR).

Initialization. Let M be the number of particles. Draw $\mathbf{b}_0^{(i)}$ from $p(\mathbf{b}_0)$ and set $w_0^{(i)} = 1/M$, $i = 1, ..., M$.

Recursive step. At time $k \geq 0$, assume that the set $\{\mathbf{b}_k^{(i)}\}_{i=1,...,M}$ is available.

1. For $i = 1, \ldots, M$,
   - (a) draw $\bar{\mathbf{b}}_{k+1}^{(i)}$ from $p(\mathbf{b}_{k+1}|\mathbf{b}_k^{(i)}, q_0)$,
   - (b) compute the weight, $\tilde{v}_{k+1}^{(i)} = p(\mathbf{o}_{k+1}|\bar{\mathbf{b}}_{k+1}^{(i)})$,
   - (c) and normalize it, $v_{k+1}^{(i)} = \frac{\tilde{v}_{k+1}^{(i)}}{\sum_{j=1}^{M} \tilde{v}_{k+1}^{(j)}}$.

2. Multinomial resampling: for $i = 1, ..., M$, assign $\mathbf{b}_{k+1}^{(i)} = \bar{\mathbf{b}}_{k+1}^{(j)}$ with probability $\bar{v}_{k+1}^{(j)}$, with $j \in \{1, ..., M\}$.

---

carried out at every k for the sake of clarity in the presentation of the algorithms. The resampled particles are all equally weighted [16], hence $v_{k+1}^{(i)} \propto p(\mathbf{o}_{k+1}|\bar{\mathbf{b}}_{k+1}^{(i)})$ independently of the i-th weight at time $k - 1$.

Let $\pi_k(d\mathbf{b}_k) = p(\mathbf{b}_k|\mathbf{o}_{1:k}, q_0)\, d\mathbf{b}_k$ denote the probability measure associated to the posterior density of $\mathbf{b}_k$. The SISR algorithm of Table 2 yields a random approximation of π_k with discrete support, namely

$$\pi_k^M(d\mathbf{b}_k) = \sum_{i=1}^{M} v_k^{(i)} \delta_{\bar{\mathbf{b}}_k^{(i)}}(d\mathbf{b}_k),$$

where $\delta_{\bar{\mathbf{b}}_k^{(i)}}$ denotes the unit delta measure centered at the point $\bar{\mathbf{b}}_k^{(i)}$ in the state-space. The measure π_k^M enables the straightforward approximation of integrals with respect to π_{k+1} as simple summations. In particular, for an arbitrary integrable function of $\mathbf{b}_k$, the integral

$$(f, \pi_k) = \int f(\mathbf{b}_k)\, \pi_k(d\mathbf{b}_k) = \int f(\mathbf{b}_k)\, p(\mathbf{b}_k|\mathbf{o}_{1:k}, q_0)\, d\mathbf{b}_k$$

is approximated as[4]

$$(f, \pi_k^M) = \int f(\mathbf{b}_k)\, \pi_k^M(d\mathbf{b}_k) = \sum_{i=1}^{M} v_k^{(i)} f(\mathbf{b}_k^{(i)}).$$

For example, the posterior mean of $\mathbf{b}_k$ given $\mathbf{o}_{1:k}$ (i.e., the minimum mean square error estimator of $\mathbf{b}_k$) can be approximated as $\hat{\mathbf{b}}_k^M = \sum_{i=1}^{M} v_k^{(i)} \bar{\mathbf{b}}_k^{(i)}$. It can be proved that $\lim_{M \to \infty}(f, \pi_k^M) = (f, \pi_k)$ in a number of ways (e.g., almost surely or in the mean square error) under mild regularity assumptions. See [35, 5] for a survey of classical results on the convergence of particle filters.

---

[4]We can also use the approximate measure $\check{\pi}_k(d\mathbf{b}_k) = \frac{1}{M} \sum_{i=1}^{M} \delta_{\mathbf{b}_k^{(i)}}(d\mathbf{b}_k)$ (built with the resampled particles) to approximate the integral (f, π_k). However, compared to (f, π_k^M), the estimator $(f, \check{\pi}_k^M)$ presents additional Monte Carlo variance due to the resampling step [16].

3.3. **Rao-Blackwellized particle filter.** The aim of this paper is the joint estimation of q_0 and tracking of $\mathbf{b}_k$. If q_0 is assumed unknown (and random), then the process of the population biomass, $\mathbf{b}_k$, is not Markov anymore, i.e., $p(\mathbf{b}_{k+1}|\mathbf{b}_{0:k}) \neq p(\mathbf{b}_{k+1}|\mathbf{b}_k, q_0)$, and the particle filter described in Table 2 can not be used.

To obtain a practical particle filter for this case, we assume again that the target density is $p(\mathbf{b}_{0:k+1}|\mathbf{o}_{1:k+1})$, with prior $p(\mathbf{b}_0)$. From Bayes' theorem we still have a recursive relationship similar to (13), namely

$$p(\mathbf{b}_{0:k+1}|\mathbf{o}_{1:k+1}) \propto p(\mathbf{o}_{k+1}|\mathbf{b}_{k+1})p(\mathbf{b}_{k+1}|\mathbf{b}_{0:k}, \mathbf{o}_{1:k})p(\mathbf{b}_{0:k}|\mathbf{o}_{1:k}),$$

where the likelihood $p(\mathbf{o}_{k+1}|\mathbf{b}_{k+1})$ does not change with respect to the case with q_0 known (the observations are still conditionally independent) but we have a factor $p(\mathbf{b}_{k+1}|\mathbf{b}_{0:k}, \mathbf{o}_{1:k})$ instead of $p(\mathbf{b}_{k+1}|\mathbf{b}_k, q_0)$.

Assume that, at time $k+1$, we can draw $\mathbf{b}_{k+1}^{(i)}$ from the distribution with pdf $p(\mathbf{b}_{k+1}|\mathbf{b}_{0:k}^{(i)}, \mathbf{o}_{1:k})$. Then, by the same argument as in Section 3.2, the normalized weight associated to $\mathbf{b}_{k+1}^{(i)}$ is still proportional to the likelihood, i.e., $v_{k+1}^{(i)} \propto p(\mathbf{o}_{k+1}|\mathbf{b}_{k+1}^{(i)})$, and we can derive a particle filter very similar in structure to the algorithm of Table 2.

Finally, we need to compute and draw from $p(\mathbf{b}_{k+1}|\mathbf{b}_{0:k}^{(i)}, \mathbf{o}_{1:k})$. This pdf can be written in terms of the random variable q_0 as

$$p(\mathbf{b}_{k+1}|\mathbf{b}_{0:k}^{(i)}, \mathbf{o}_{1:k}) = \int p(\mathbf{b}_{k+1}|\mathbf{b}_k^{(i)}, q_0)\, p(q_0|\mathbf{b}_{0:k}^{(i)})\, dq_0, \tag{16}$$

by exploiting the fact that $p(\mathbf{b}_{k+1}|\mathbf{b}_{1:k}^{(i)}, \mathbf{o}_{1:k}, q_0) = p(\mathbf{b}_{k+1}|\mathbf{b}_k^{(i)}, q_0)$, since the sequence $\mathbf{b}_k$ is Markov conditional on q_0, and $p(q_0|\mathbf{b}_{0:k}^{(i)}, \mathbf{o}_{1:k}) = p(q_0|\mathbf{b}_{0:k}^{(i)})$, since q_0 is independent of the observations $\mathbf{o}_{1:k}$ given the sequences of biomass $\mathbf{b}_{0:k}^{(i)}$.

However, conditional on the sequence $\mathbf{b}_{0:k}^{(i)}$, the estimation of q_0 can be addressed by means of the linear-Gaussian state space model of Section 2.2 and solved numerically using the simple Kalman filtering algorithm of Table 1. In particular, if we define $\Delta_{k+1}^{(i)}$, $\mathbf{h}_{k+1}^{(i)}$, $\mathbf{Q}_{k+1}^{(i)}$, $\mathbf{g}_{k+1}^{(i)}$ and $\mathbf{z}_{k+1}^{(i)}$ exactly in the same way as in Section 2.2 but using the biomass vector $\mathbf{b}_k^{(i)} = [x_k^{(i)}, y_k^{(i)}]^\top$ instead of the generic x_k and y_k of Eq. (5), then $p(q_0|\mathbf{b}_{0:k}^{(i)}) = p(q_0|\mathbf{z}_{1:k}^{(i)})$, which can be computed exactly using the Kalman filter to obtain

$$p(q_0|\mathbf{b}_{0:k}^{(i)}) = \mathcal{N}(q_0; \hat{q}_{0,k}^{(i)}, P_k^{(i)}). \tag{17}$$

The superscript $^{(i)}$ in the posterior mean and variance of q_0 indicates that they both depend on the particle $\mathbf{b}_{0:k}^{(i)}$. Since the PF handles a set of M particles, this means that a bank of M Kalman filters running in parallel has to be implemented.

Both $p(q_0|\mathbf{b}_{0:k}^{(i)})$ and $p(\mathbf{b}_{k+1}|\mathbf{b}_k^{(i)}, q_0)$ are Gaussian (see Eqs. (17) and (9), respectively) and, as a consequence, the integral in (16) also yields a Gaussian density (see, e.g., [11]). In particular, it can be shown that

$$p(\mathbf{b}_{k+1}|\mathbf{b}_{0:k}^{(i)}, \mathbf{o}_{1:k}) = \mathcal{N}(\mathbf{b}_{k+1}; \boldsymbol{\beta}_{k+1}^{(i)}, \mathbf{B}_{k+1}^{(i)}), \tag{18}$$

where

$$\boldsymbol{\beta}_{k+1}^{(i)} = \mathbf{g}_{k+1}^{(i)} \hat{q}_{0,k}^{(i)} + \mathbf{b}_k^{(i)} + \mathbf{h}_{k+1}^{(i)}, \quad \text{and}$$

$$\mathbf{B}_{k+1}^{(i)} = \mathbf{g}_{k+1}^{(i)} P_k^{(i)} \mathbf{g}_{k+1}^{(i)\top} + \tau \mathbf{Q}_{k+1}^{(i)} \mathbf{Q}_{k+1}^{(i)\top}.$$

TABLE 3. Rao-Blackwellized PF for biomass tracking when the functional response parameter q_0 is unknown.

Initialization. Draw $\mathbf{b}_0^{(i)}$, $i = 1, ..., M$, from the prior pdf $p(\mathbf{b}_0)$. Select the prior mean, $\hat{q}_{0,0}$, and variance, P_0, for the unknown parameter q_0. Set $\hat{q}_{0,0}^{(i)} = \hat{q}_{0,0}$ and $P_0^{(i)} = P_0$ for each $i = 1, ..., M$.

Recursive step. At time $k \geq 0$, assume that the set $\left\{ \mathbf{b}_{0:k}^{(i)}, \hat{q}_{0,k}^{(i)}, P_k^{(i)} \right\}_{i=1,...,M}$ is available. Then proceed as follows.

  1. For each $i = 1, ..., M$:

    (a) Draw $\bar{\mathbf{b}}_{k+1}^{(i)}$ from the Gaussian pdf $\mathcal{N}(\mathbf{b}_{k+1}; \boldsymbol{\beta}_{k+1}^{(i)}, \mathbf{B}_{k+1}^{(i)})$ specified in Eq. (18).

    (b) Compute the weight $\tilde{v}_{k+1}^{(i)} = p(\mathbf{o}_{k+1}|\bar{\mathbf{b}}_{k+1}^{(i)})$ according to Eq. (10).

    (c) Normalize the weight as $v_{k+1}^{(i)} = \frac{\tilde{v}_{k+1}^{(i)}}{\sum_{j=1}^{M} \tilde{v}_{k+1}^{(j)}}$.

    (d) Update the posterior pdf of q_0 conditional on $\{\bar{\mathbf{b}}_{k+1}^{(i)}, \mathbf{b}_{0:k}^{(i)}\}$ by taking one step of the Kalman filter outlined in Table 1. Obtain
$p(q_0|\bar{\mathbf{b}}_{k+1}^{(i)}, \mathbf{b}_{0:k}^{(i)}) = \mathcal{N}(q_0; \hat{q}_{0,k+1}^{(i)}, P_{k+1}^{(i)})$.

  2. Multinomial resampling: for $i = 1, ..., M$, let $\mathbf{b}_{0:k+1}^{(i)} = \{\bar{\mathbf{b}}_{k+1}^{(j)}, \mathbf{b}_{0:k}^{(j)}\}$, $\hat{q}_{0,k+1}^{(i)} = \hat{q}_{0,k+1}^{(j)}$ and $P_{k+1}^{(i)} = P_{k+1}^{(j)}$ with probability $v_{k+1}^{(j)}$, $j \in \{1, ..., M\}$.

Table 3 outlines the proposed PF for tracking the biomass in $\mathbf{b}_k$ with unknown parameter q_0. As in the case of the basic PF of Table 2, it includes a multinomial resampling step at every time k. Specifically notice that, after resampling, it is necessary to keep track of the Kalman filter outputs (mean and variance) for each particle.

A posterior estimate of q_0 can be easily obtained at any time k using the statistics generated by the algorithm of Table 3. In particular, the posterior mean and variance of q_0 conditional on the observations $\mathbf{o}_{1:k}$ can be approximated as

$$\hat{q}_{0,k}^M = \sum_{i=1}^{M} v_k^{(i)} \hat{q}_{0,k}^{(i)}, \tag{19}$$

$$P_k^M = \sum_{i=1}^{M} v_k^{(i)} \left[\left(\hat{q}_{0,k}^{(i)} - \hat{q}_{0,k}^M \right)^2 + P_k^{(i)} \right], \tag{20}$$

respectively.

The proposed algorithm, outlined in Table 3, is an example of a Rao-Blackwellized particle filter (RBPF) [11, 16]. Compared to other particle filtering methods where the unknown functional-response parameters are approximated by sampling [32, 19, 18], the RBPF has as a key feature the analytical integration of q_0 by way of a bank of Kalman filters. This is possible, because of the conditionally linear (and Gaussian) structure of the Lotka-Volterra system given the sequences of biomass, as explicitly displayed by Eq. (6). Handling q_0 analytically reduces both the dimension of the state space where particles have to be generated and the variance of the estimators (both of q_0 and $\mathbf{b}_k$) [11, 16]. Moreover, the derivation of the algorithm

TABLE 4. Rao-Blackwellized PF for biomass tracking with unknown q_0 and missing data.

Let $\mathcal{K} \subseteq \{1, 2, \ldots, S\}$ be the set of discrete time instants in which observations are available.

Initialization. Draw $\mathbf{b}_0^{(i)}$, $i = 1, ..., M$, from the prior pdf $p(\mathbf{b}_0)$. Select the prior mean, $\hat{q}_{0,0}$, and variance, P_0, for the unknown parameter q_0. Set $\hat{q}_{0,0}^{(i)} = \hat{q}_{0,0}$ and $P_0^{(i)} = P_0$ for each $i = 1, ..., M$.

Recursive step. At every $k \geq 0$, assume that the set $\left\{ \mathbf{b}_{0:k}^{(i)}, \hat{q}_{0,k}^{(i)}, P_k^{(i)} \right\}_{i=1,...,M}$ is available. Then proceed as follows.

1. For each $i = 1, ..., M$:

   (a) Draw $\bar{\mathbf{b}}_{k+1}^{(i)}$ from the Gaussian pdf $\mathcal{N}(\mathbf{b}_{k+1}; \boldsymbol{\beta}_{k+1}^{(i)}, \mathbf{B}_{k+1}^{(i)})$ specified in Eq. (18).

   (b) Update the posterior pdf of q_0 conditional on $\{\bar{\mathbf{b}}_{k+1}^{(i)}, \mathbf{b}_{0:k}^{(i)}\}$ by taking one step of the Kalman filter outlined in Table 1. Obtain
   $p(q_0 | \bar{\mathbf{b}}_{k+1}^{(i)}, \mathbf{b}_{0:k}^{(i)}) = \mathcal{N}(q_0; \hat{q}_{0,k+1}^{(i)}, P_{k+1}^{(i)})$.

2. If $k \in \mathcal{K}$, then:

   (a) For each $i = 1, ..., M$: compute the weight $\tilde{v}_{k+1}^{(i)} = p(\mathbf{o}_{k+1} | \bar{\mathbf{b}}_{k+1}^{(i)})$ according to Eq. (10) and normalize the weight as $v_{k+1}^{(i)} = \frac{\tilde{v}_{k+1}^{(i)}}{\sum_{j=1}^{M} \tilde{v}_{k+1}^{(j)}}$.

   (b) Resample: for $i = 1, ..., M$, let $\mathbf{b}_{0:k+1}^{(i)} = \{\bar{\mathbf{b}}_{k+1}^{(j)}, \mathbf{b}_{0:k}^{(j)}\}$, $\hat{q}_{0,k+1}^{(i)} = \hat{q}_{0,k+1}^{(j)}$ and $P_{k+1}^{(i)} = P_{k+1}^{(j)}$ with probability $v_{k+1}^{(j)}$, $j \in \{1, ..., M\}$.

---

is rigorous and asymptotic convergence is guaranteed in a similar way as for the standard PF[5].

3.4. **Rao-Blackwellized particle filtering with missing observations.** Real data regarding the population biomass are often not available at each discrete time instant k. The proposed RBPF algorithm can also be applied in this case[6], with the only constrain that the importance weights can only be updated at the times when data are available. Since the role of the resampling step is to avoid the degeneracy of the weights, it is only needed when the weights are updated. As before, we assume a multinomial resampling scheme.

Table 4 outlines the RBPF algorithm with missing observations. We assume that observations are available at L ordered time instants $k_1, k_2, \ldots, k_L$ with $k_1 \geq 1$ and $k_L \leq S$. The set of instants with available data is denoted with $\mathcal{K} = \{k_1, k_2, \ldots, k_L\} \subseteq \{1, 2, \ldots, S\}$.

4. **Case study.** We apply the proposed RBPF method (Table 4) to the acarine predator-prey system studied in [23]: the prey mite *Tetranychus urticae* and the

---

[5]For example, Lemma 1 in [34] is general enough to guarantee the convergence of the RBPF algorithm described herein.

[6]We can also apply the proposed RBPF method when only observations of the prey population are available. Our computer simulation results (not shown in the paper) indicate that the unknown parameter q_0 is estimated accurately and the two population biomasses are tracked with an error not much higher than in the full observation case.
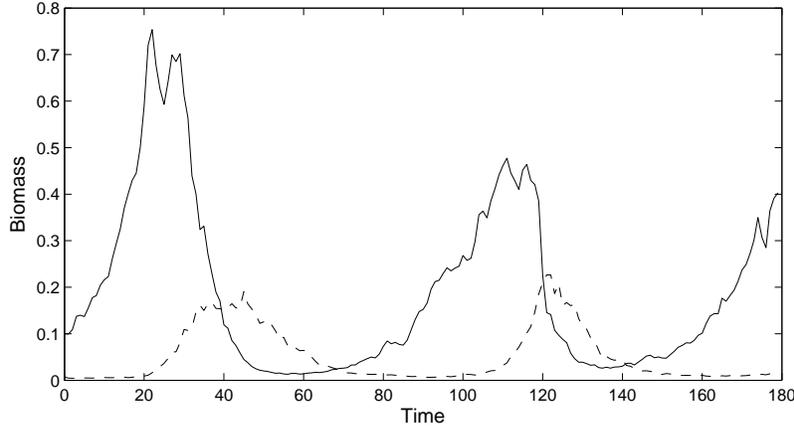
FIGURE 1. Synthetic series of the prey (continuous line) and predator (dashed line) biomass, with $x_0 = 0.1$, $y_0 = 0.007$ and $q_0 = 1.5$.

predator mite *Phytoseiulus persimilis*. The population dynamics is described by Eq. (2) where the behavioral parameter q_0 is unknown.

The parameter values are as follows

$$r = 0.11, c = 0.35, u = 0.09, \sigma = 0.321, \varepsilon = 0.079 \quad \text{and} \eta = 0.106$$

according to [23]. The initial conditions are $x_0 = 0.1$, $y_0 = 0.007$, the period τ between consecutive observations is equal to 1 and expressed in days, and the final time is $S = 179$ days. In Section 4.1 the algorithm is tested using synthetic data and, then, in Section 4.2, it is validated on a set of field data. Finally, the proposed RBPF is compared with the MCMC method of [23] in Section 4.3.

4.1. **Synthetic data.** In order to generate a synthetic dataset, we set $q_0 = 1.5$. Then we use the model in Eq. (2) to generate a sequence of prey $x_{1:S}$ and predator $y_{1:S}$ population biomass values. The two sequences are displayed in Figure 1. From these complete sequences, we generate $L = 10$ noisy observations, $\mathbf{o}_{k_1}, \ldots, \mathbf{o}_{k_L}$. Each scalar observation $o_{k_i}^x$ or $o_{k_i}^y$ with $i = 1, ..., L$ is a gamma random variate with mean equal to the corresponding population biomass and variance 10^{-4}.

We have applied the RBPF algorithm with $M = 10^5$ particles to jointly estimate the unknown parameter q_0 and track the prey and predator biomass given the available set of $L = 10$ synthetic observations. All particles are initialized in the same way (i.e., the prior of the random vector $\mathbf{b}_0$ is a delta measure), $x_0 = 0.1362$ and $y_0 = 0.0004$ are set, and a Gaussian distribution is assumed for the prior density of q_0[7] with $\hat{q}_{0,0} = 0$ and $P_0 = 1$.

---

[7]The parameter q_0 represents the feeding rate of the predators, hence it cannot be negative in practice. However, the proposed methods demand that the prior $p(q_0)$ be Gaussian for formal consistency. With this constraint in mind, the choice of $\mathcal{N}(q_0; 0, 1)$ appears poor, because a large prior probability is assigned to negative values of q_0. A prior with positive mean $\hat{q}_{0,0} > 0$ can be used as well without any modification of the procedure. However, even with $\hat{q}_{0,0} = 0$, the inference algorithm performs well (no artifacts, in the form of negative estimates of q_0 are observed); hence, we have chosen to use this "poor" prior to illustrate the robustness of the method.

We have worked with different values of the observation variance, $d_x^2 = d_y^2$ (see Eq. (10)) in order to perform a sensitivity analysis on the parameter q_0, assessing the robustness of the proposed approach upon the unknown variance. For each value of the observation variance we have obtained an approximate posterior distribution of the parameter q_0. Note that every posterior distribution generated by the RBPF has the form of a mixture of Gaussian distributions, namely

$$\hat{p}^M(q_0|\mathbf{o}_{k_1:k_L}) = \sum_{i=1}^{M} v_S^{(i)} \mathcal{N}(q_0; \hat{q}_{0,S}^{(i)}, P_S^{(i)}). \tag{21}$$

In order to assess the quality of the approximate densities, we have generated 100 random draws, denoted with q_0^j where $j = 1, ..., 100$, from each density. Then, for each draw q_0^j, we have generated 5 independent sequences of prey and predator biomass, denoted with $\{\tilde{x}_{0:S}^{j,m}, \tilde{y}_{0:S}^{j,m}\}$ where $m = 1, ..., 5$ using the model of Eq. (2). All of them have the same starting points $\tilde{x}_0^{j,m} = 0.1362$ and $\tilde{y}_0^{j,m} = 0.0004$).

Let $\tilde{x}_{0:S}$ and $\tilde{y}_{0:S}$ be the average of all the sequences of population biomass, i.e.,

$$\tilde{x}_k = \frac{1}{500} \sum_{m=1}^{5} \sum_{j=1}^{100} \tilde{x}_k^{j,m} \quad \text{and} \quad \tilde{y}_k = \frac{1}{500} \sum_{m=1}^{5} \sum_{j=1}^{100} \tilde{y}_k^{j,m},$$

with $k = 0, ..., S$. We compare the population estimates with the observations $\mathbf{o}_k = [o_k^x, o_k^y]^\top$ with ($k \in \mathcal{K}$) by means of a normalized error consisting of the sum of squared errors (at the times where real observations are available) over the empirical variance of the data. To be specific, we define the normalized sum of squares error (NSSE) for the prey and predator biomass, respectively, as follows[8]

$$NSSE_x = \frac{\sum_{k\in\mathcal{K}}(o_k^x - \tilde{x}_k)^2}{\sum_{k\in\mathcal{K}}(o_k^x - \bar{o}^x)^2} \tag{22}$$

$$NSSE_y = \frac{\sum_{k\in\mathcal{K}}(o_k^y - \tilde{y}_k)^2}{\sum_{k\in\mathcal{K}}(o_k^y - \bar{o}^y)^2} \tag{23}$$

where $\bar{o}^x = \frac{1}{L}\sum_{k\in\mathcal{K}} o_k^x$ and $\bar{o}^y = \frac{1}{L}\sum_{k\in\mathcal{K}} o_k^y$. The methodology is the same as the one used for the evaluation of the inference algorithm with field data in Section 4.2.

The results of the evaluation of $NSSE_x$ and $NSSE_x$ for each observation variance are displayed in Table 5. We observe that the NSSE attains its minimum value when $d_x^2 = d_y^2 = 10^{-4}$, which yields posterior mean and variance approximations $\hat{q}_{0,S}^M = 1.4985$ and $P_S^M = 0.0128$, respectively.

Figure 2 shows the evaluation of the posterior mean $\hat{q}_{0,k}^M$ with $k = 1, ..., S$, generated by the RBPF method with $d_x^2 = d_y^2 = 10^{-4}$ and $M = 10^5$ (see Eq. (19)). The steps are due to the missing data (i.e., the value $\hat{q}_{0,k}^M$ changes most significantly when a new datum is processed and the weights are updated).

Since particle filters are sequential algorithms, it is possible to obtain estimates of the biomass online at each time k. For the same simulation of Figure 2, Figure

---

[8]Since the biomass is time varying and can occasionally take either very large or very small values, a "direct" error of the form, e.g., $\sum_{k\in\mathcal{K}} |o_k^x - \tilde{x}_k|$ can be misleading. Indeed, if o_k^x is close to 0, an error of 300% in the estimator $\tilde{x}_k$ can still be perceived as "small". On the contrary, if o_k^x takes a very high value, errors of, say, 0.01% can still seem "large". To avoid these artifacts, we will assess performance by way of a normalized error. Intuitively, the effect of the normalization is to "amplify" the errors when the data are very stable (with small fluctuations) while "tempering" them when the data presents large variability.

TABLE 5. Performance of the RBPF algorithm with synthetic data, $M = 10^5$ and several values of the observation variance $d_x^2 = d_y^2$. The NSSE values are calculated over the average of 500 sequences of prey and predator biomass generated with 100 independent draws from the approximate posterior of q_0 obtained from the particle filter.

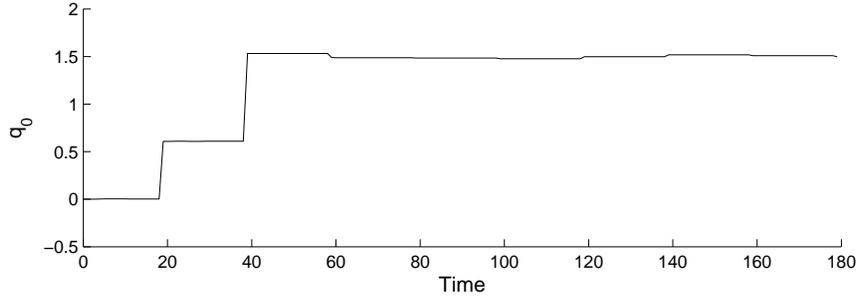| Observation variance	$\hat{q}_{0,S}^M$	P_S^M	$NSSE_x$	$NSSE_y$
10^{-8}	1.4779	0.0045	0.4530	0.5174
10^{-7}	1.4292	0.0043	0.4523	0.5028
10^{-6}	1.5139	0.0056	0.4283	0.4949
10^{-5}	1.4619	0.0079	0.4152	0.4897
10^{-4}	1.4985	0.0128	0.4084	0.4694
10^{-3}	1.4701	0.0165	0.4616	0.5152

FIGURE 2. Particle filter estimates $(\hat{q}_{0,k}^M, \; k = 1, 2, ..., S)$ of the unknown parameter q_0 over time with $M = 10^5$ particles.

3 displays the true (synthetic) sequences $x_{0:S}$ and $y_{0:S}$ together with the online estimates

$$\hat{x}_k^M = \sum_{i=1}^M v_k^{(i)} x_k^{(i)} \quad \text{and} \quad \hat{y}_k^M = \sum_{i=1}^M v_k^{(i)} y_k^{(i)}. \tag{24}$$

The biomass sequences at the instants $k_1, \ldots, k_L$ where observations are actually available are displayed with stars. It can be seen that the estimates are accurate at the times where observations are processed, but there is a drift (the error increases) when data are not available, especially for $k < 40$. From Figure 2 we also see that for $k \geq 40$ the estimates of q_0 are more accurate, and this also affects the accuracy of the biomass estimation.

We use $M = 10^5$ particles to guarantee a good estimation of the biomass variables, stable across different simulation runs. In order to assess the stability of the filter and the "balance" of the particle set, it is customary to estimate the effective sample size (ESS) as [16]

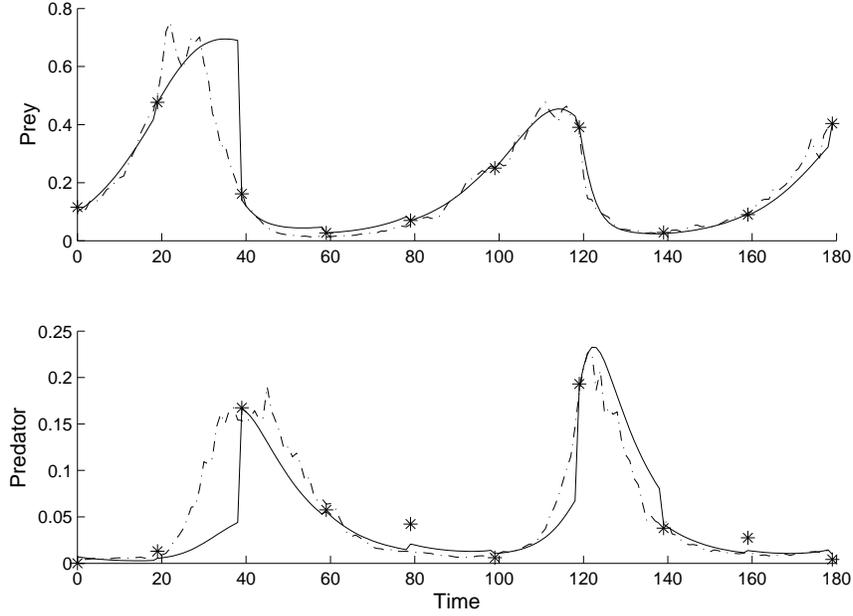$$\hat{M}_{eff} = \frac{1}{\sum_{i=1}^M \left(v_k^{(i)} \right)^2}. \tag{25}$$

FIGURE 3. Comparison of the true synthetic biomass sequences (dash-dotted lines) and the online biomass estimates (continuous lines) generated by the RBPF algorithm of Table 4. The points for which observations are available are displayed with stars.

A small value of $\hat{M}_{eff}$ means a large variance for the weights, hence a stronger degeneracy. Figure 4 shows the $\hat{M}_{eff}$ values obtained over time. The ESS is piece-wise constant because the weights only change when new observations become available. According to the results, the filter is stable most of the time, with a reasonable diversity and only at $k = 40$ and $k = 120$ it drops because the lack of observations in the previous time steps makes it difficult to keep the quality of the particle set.

Better tracking results are obtained when the biomass sequences are estimated with a second "pass" of the particle filter. To show it, we have taken the estimate $\hat{q}_{0,S}^M = 1.4985$ generated by the RBPF with the lowest $NSSE_x$ and $NSSE_y$ (Table 4) and then run the simpler PF of Table 2 with $M = 10^5$ and fixed $q_0 = 1.4985$ using the same set of 10 observations. We have selected the same initial conditions, $x_0 = 0.1362$ and $y_0 = 0.0004$, $\tau = 1$ day, and observation variance $d_x^2 = d_y^2 = 10^{-4}$ in Eq. (10). The results, plotted in Figure 5 show a clear improvement in the biomass estimates for $1 \leq k \leq 40$.

4.2. **Field data.** The data used in this subsection concern the dynamics of the acarine predator-prey system *Tetranychus urticae-Phytoseiulus persimilis* and have been collected in a strawberry crop in Ispica (Ragusa, Italy) [25].

The series consists of $L = 13$ data samples over a time interval of $S = 98$ days. In [23], 6 observations of this dataset (from 2nd to 7th in the time series), which represent the first cycle of the prey, were used to estimate the unknown parameter
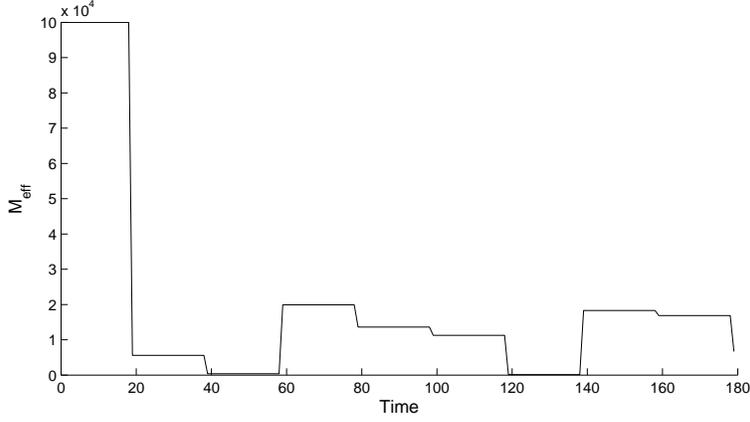
FIGURE 4. The effective sample size, $\hat{M}_{eff}$, estimated over time for a typical run of the RBPF algorithm with the setup of Section 4.1.
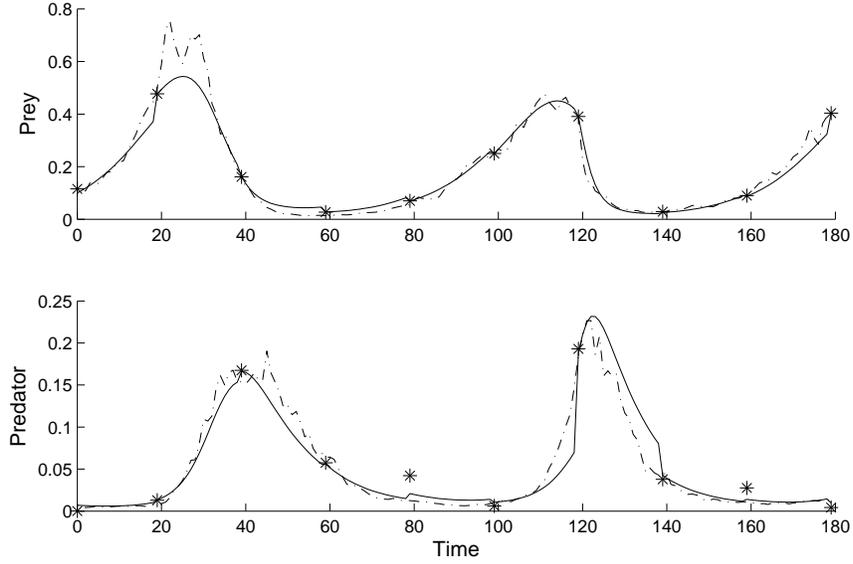

FIGURE 5. Comparison of the true synthetic biomass sequences (dash-dotted lines) and the online biomass estimates (continuous lines) generated by the PF of Table 2 with fix $q_0 = 1.4985$. The points for which observations are available are displayed with stars.

q_0. We take the complete dataset together with the final time $S = 98$ days. Our goal is to forecast the prey and predator biomass between consecutive field data and to estimate the unknown parameter q_0.

TABLE 6. Performance of the RBPF algorithm with field data, $M = 2 \times 10^5$ particles and several values of the observation variance $d_x^2 = d_y^2$. The NSSE values are calculated over the average of 500 sequences of prey and predator biomass generated with 100 independent draws from the approximate posterior of q_0 obtained from the particle filter. Results are shown for a small dataset ($S = 49$ days, 7 field data samples) and the complete dataset ($S = 98$ days, 13 field data samples).

	Observation variance	$\hat{q}_{0,S}^M$	P_S^M	$NSSE_x$	$NSSE_y$
$S = 49$	$\leq 10^{-7}$	-	-	-	-
	10^{-6}	1.6570	0.0105	0.2307	0.0544
	10^{-5}	1.6715	0.0134	0.2082	0.0446
	10^{-4}	1.6985	0.0137	0.1839	0.0441
$S = 98$	$\leq 10^{-7}$	-	-	-	-
	10^{-6}	1.7283	0.0093	0.1334	0.1569
	10^{-5}	1.8464	0.0096	0.1116	0.1361
	10^{-4}	1.9417	0.0097	0.1253	0.1557

We have run the RBPF algorithm of Table 4 with $M = 2 \times 10^5$ particles and field observations. The same as in the experiments with synthetic data, we set initial conditions $x_0 = 0.1362$ and $y_0 = 0.0004$ (for all particles), a time period $\tau = 1$ day, and a Gaussian prior $p(q_0) = \mathcal{N}(q_0; 0, 1)$. The measurement error is unknown, thus we have run the RBPF algorithm using different observation variances starting from low values. For each value of the observation variance, we have obtained an approximate posterior distribution of q_0 (see Eq. (21)) and in order to assess the validity of the approximation we have followed the same methodology as in the computer simulations whose results are displayed in Table 5.

The results of the experiment with field data are shown in Table 6. In this table, both intermediate results, by setting the observation period to only $S = 49$ days (this includes 7 field data samples), and results for the complete field dataset ($S = 98$, 13 data samples) are displayed.

It is observed that the estimation error of the prey estimates ($NSSE_x$) is slightly lower when processing the complete dataset ($NSSE_x = 0.1839$ for $d_x^2 = d_y^2 = 10^{-4}$ with $S = 49$, while $NSSE_x = 0.1116$ for $d_x^2 = d_y^2 = 10^{-5}$ with $S = 98$). However, the error of the predator estimates is clearly lower for the short sequence of field data ($NSSE_y = 0.0441$ for $d_x^2 = d_y^2 = 10^{-4}$ with $S = 49$, while $NSSE_y = 0.1361$ for $d_x^2 = d_y^2 = 10^{-5}$ with $S = 98$). It should also be noticed that the errors are minimized for observation variance 10^{-4} with $S = 49$, while for $S = 98$ the best results correspond to variance 10^{-5}.

Figure 6 shows the evolution of the posterior mean estimates of the unknown parameter $\hat{q}_{0,k}^M$ (with $k = 1, \ldots, 98$) using the observation variance $d_x^2 = d_y^2 = 10^{-5}$ and the field dataset. We have used the same number of particles, initial conditions and prior $p(q_0)$ as before ($M = 2 \times 10^5$, $x_0 = 0.1362$, $y_0 = 0.0004$, $p(q_0) = \mathcal{N}(q_0; 0, 1)$). The same step shape as in Figure 2 is observed, with jumps associated to the time instants when observations are available. For $k \geq 57$, the estimate $\hat{q}_{0,k}^M$ is already close to its final value $\hat{q}_{0,S}^M$.
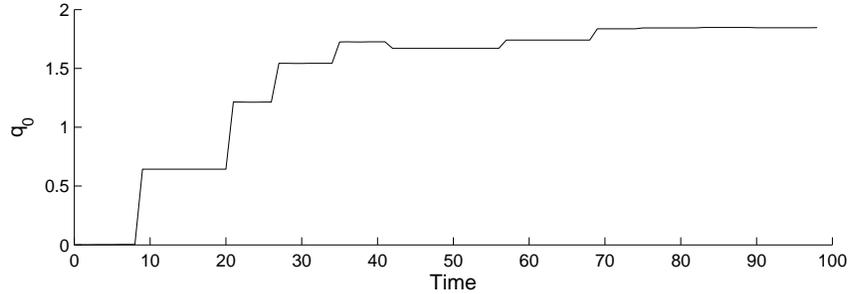
FIGURE 6. Particle filter estimates ($\hat{q}_{0,k}^M$, $k = 1, 2, ..., 98$) of the unknown parameter q_0 over time with $M = 2 \times 10^5$ particles, the observation variance $d_x^2 = d_y^2 = 10^{-5}$ and field data.

Figure 7 compares the field observations (marked with stars) and the online estimates (computed as in Eq. (24)) for the same experiment as in Figure 6. We observe some apparent misadjustment in the estimation of the predator biomass in the four initial data points (i.e., until $k = 30$, approximately). This fact is not surprising because: (a) the parameter estimate has not converged yet at this time (see Figure 6) and (b) the predator population appears to be extremely low, which makes tracking more difficult. Starting from the fourth point, both populations are estimated accurately, until the predator population becomes very low again at the end of the time period.

We have also applied the PF of Table 2, with $M = 2 \times 10^5$ particles and fixed $q_0 = 1.8464$, to the field data in order to obtain a more reliable forecast of the sequences of biomass, especially for the first part of the time period. As in the previous experiments, we set $x_0 = 0.1362$, $y_0 = 0.0004$, $\tau = 1$ and $d_x^2 = d_y^2 = 10^{-5}$. The results are shown in Figure 8. The predator biomass estimation is improved from $k = 9$ to $k = 35$, while the estimates of the prey biomass are very similar to the online estimates generated by the RBPF algorithm.

The RBPF algorithm with $M = 2 \times 10^5$ particles, coded as a Matlab (version 7.6, R2008a) script, runs in ≈ 18.6 minutes on an Intel Core2 Quad Q9300 2.50GHz processor for the large dataser ($S = 98$). We remark that if new data were to be collected the required computation time would be proportional to the length of the *new* dataset only, since the new approximation of the posterior distribution (of both q_0 and the biomasses) would be computed recursively. This is in contrast with MCMC methods, which would require to re-process the old data as well.

4.3. **Comparison with the method of** [23]. In this section, we compare the particle filtering method introduced in this paper and the MCMC technique proposed in [23]. We are interested in assessing the quality of the estimates of the parameter q_0 generated by the two methodologies. The posterior mean and variance of q_0 obtained via the RBPF are 1.8464 and 0.0096, respectively, while the posterior mean and variance obtained via the MCMC technique of [23] are 1.6863 and 0.0026, respectively.

A direct evaluation of the estimation accuracy is impossible because a "true" value of q_0 is unknown. Therefore, we carry out an indirect comparison by way of
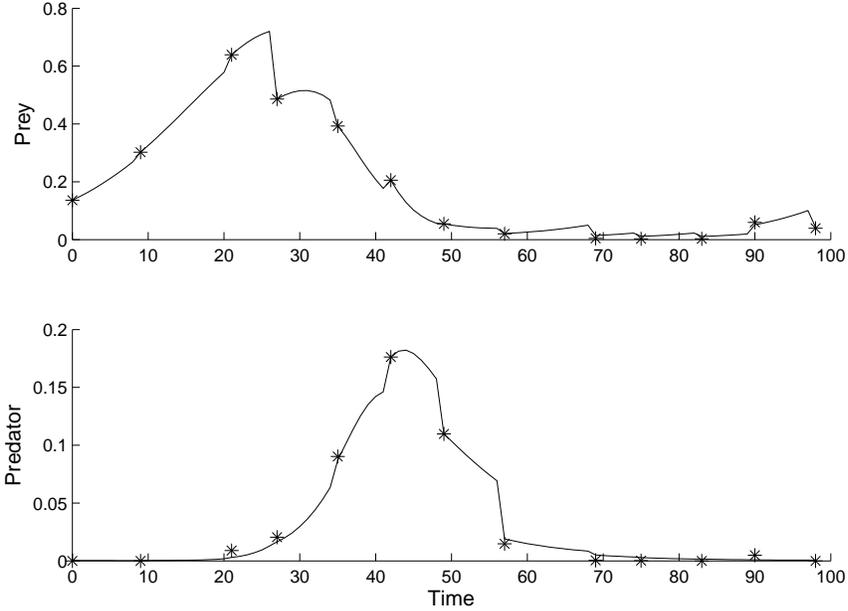
FIGURE 7. Online estimates of the prey and predator biomass (continuous line) and field data points (stars). These results have been obtained with the RBPF of Table 4, with $M = 2 \times 10^5$ particles.

the NSSE of both the prey and the predator biomass[9]. In particular, we follow the same methodology as to obtain the results of Table 5.

Tables 7 and 8 display the values of the field data samples for the prey and the predator, respectively, together with the mean values (at the same time instants) corresponding to draws from the approximate posterior distribution of q_0 obtained from the RBPF algorithm and from the MCMC algorithm of [23]. Table 9 displays the NSSE values attained by both methodologies (MCMC in [23] and the RBPF algorithm in this paper). The approximate posterior of q_0 obtained via the RBPF algorithm yields lower values of the NSSE both for the prey and the predator, both with the short field data series ($S = 49$) and the long field data series ($S = 98$).

According to the NSSE comparison in Table 9, the RBPF algorithm yields a better approximation of the posterior distribution of q_0 (hence, better estimates) than the MCMC method of [23]. Moreover, the technique herein proposed allows to improve the forecast of population dynamics, because it enables the assimilation of new data samples as they become available. In particular, the MCMC methodology was used to obtain a single estimation based on the entire dataset, while the proposed RBPF technique is also useful in case an estimate of the parameter and a

---

[9]In the case of the predator time series, to calculate $NSSE_y$ values we use estimations and experimental data from the 3rd to the 13th in the time series because there are not MCMC estimations for 1st and 2nd observations. This is because the MCMC method of [23] does not allow us to handle null observations.
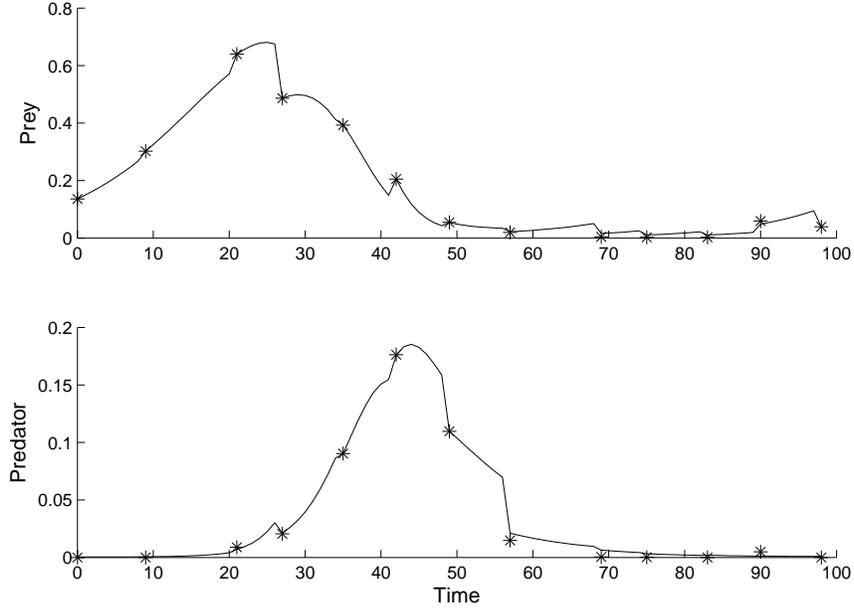
FIGURE 8. Estimates of the prey and predator biomass obtained with the particle filter of Table 2 with $M = 2 \times 10^5$ particles and fix $q_0 = 1.8464$. Asterisks denote experimental data.

TABLE 7. Comparison of prey experimental biomass and mean biomass from 500 independent simulations of model (2) using 100 random draws of q_0 from the posterior approximated via MCMC [23] and from the posterior approximated via the RBPF algorithm.

Time	Experimental biomass	with q_0 from MCMC	with q_0 from RBPF
0	0.1362	0.1362	0.1362
9	0.3024	0.2956	0.2861
21	0.6393	0.5999	0.5688
27	0.4863	0.5934	0.6366
35	0.3930	0.2551	0.3860
42	0.2053	0.0942	0.1144
49	0.0545	0.0484	0.0366
57	0.0198	0.0405	0.0205
69	0.0045	0.0581	0.0306
75	0.0026	0.0796	0.0433
83	0.0028	0.1202	0.0694
90	0.0595	0.1654	0.1069
98	0.0394	0.2203	0.1597

TABLE 8. Comparison of predator experimental biomass and mean biomass from 500 independent simulations of model (2) using 100 random draws of q_0 from the posterior approximated via MCMC [23] and from the posterior approximated via the RBPF algorithm.

Time	Experimental biomass	with q_0 from MCMC	with q_0 from RBPF
0	0	-	0.0004
9	0	-	0.0006
21	0.0089	0.0089	0.0049
27	0.0205	0.0467	0.0262
35	0.0903	0.1560	0.1304
42	0.1763	0.1425	0.1669
49	0.1097	0.0981	0.1150
57	0.0148	0.0588	0.0627
69	0.0005	0.0275	0.0239
75	0.0002	0.0212	0.0159
83	0	0.018	0.0109
90	0.0049	0.0204	0.0099
98	0	0.0277	0.0133

TABLE 9. Comparison of the NSSE for the prey ($NSSE_x$) and the predator ($NSSE_y$) obtained from random draws of q_0 using the approximate posterior distributions generated by the MCMC method of [23] and the RBPF algorithm in this paper.

	First cycle		Complete series	
	$NSSE_x$	$NSSE_y$	$NSSE_x$	$NSSE_y$
MCMC [23]	0.1760	0.3331	0.2075	0.3018
RBPF (Table 4)	0.1443	0.0941	0.1116	0.1459

foresight of prey and/or predator biomass are required during the evolution of the populations.

5. **Discussion.** In this paper we have investigated a particle filtering method for estimating the functional response and tracking population biomass in a stochastic predator-prey system. The system is described by a Lotka-Volterra type model with logistic growth of the prey as proposed in [23]. The linear structure of the Lotka-Volterra functional response conditional on the population biomass allows to design an efficient particle filtering technique. The proposed method uses a bank of Kalman filters for analytically integrating the unknown parameter, while sampling in the 2-dimensional space of the prey and predator biomass. Compared to other particle filtering techniques that use Monte Carlo sampling for estimating the unknown parameter, the proposed approach reduces the variance of the resulting estimates.

Then, this particle filter method is adapted to small observation datasets, updating importance weights and resampling the particle set only when experimental observations become available. These characteristics make the method suitable for adaptive management. In fact, according to the adaptive management framework, information synthesis is performed with models whose parameters are continuously

adapted to the level of available information. We agree with [41] on the utility of an adaptive management framework in integrated pest management (IPM). Within the adaptive management framework in IPM, the predator-prey model we propose can undergo changes leading to improved predictive and explicative capabilities as more information becomes available.

The use of the Lotka-Volterra model should represent a limitation due to the underlying biology. The conditionally linear functional response in the model implies an unsaturated capability of prey biomass intake for the predator. In pest management context, in most of the cases we are interested in short or medium-term forecast, and for predator-prey dynamics the time-frame usually comprises no more than a single population cycle. In this condition the intrinsic limitation in the conditionally linear functional response model is outpaced by the advantages offered by the availability of prompt and progressively improved estimation of the predator functional response.

The proposed method enables us to jointly estimate the functional response and the biomass of prey and predator. For testing the behavior of the particle filter algorithm, we have used both a set of synthetic data and experimental observations of an acarine predator-prey system, the pest mite *Tetranychus urticae* and the predator mite *Phytoseiulus persimilis*. The estimated distribution of q_0 and mean trajectories of predator and prey show a satisfactory fit to field data. This result confirms the goodness of the proposed method.

We would like to point out that, differently from MCMC methods, the PF method does not present restriction on the dataset. In fact, it can be applied also during the period of data collection without waiting up to the end of at least one cycle of the population like in [23]. This aspect is very important in the design of strategies of predator release for biological control.

An additional strength of the proposed RBPF algorithm is that it can be easily integrated with some computational methodologies, recently proposed in the statistics literature, that are clearly susceptible of future application to the problems involving parameter estimation in predator-prey models. This particularly includes PMCMC [3] and sequential Monte Carlo square (SMC^2) [12] techniques. For example, one can think of a SMC^2 algorithm for the joint estimation of several model parameters (e.g., ε, σ or η in Eq. (2)) beyond the functional response. In such algorithm, the proposed RBPF would allow to to analytically handle the behavioral parameter q_0 in the second layer of filters of the SMC^2 scheme. In this way, the conditionally-linear structure of the model on q_0 would still be exploited and the dimension of the sampling space would not be unnecessarily increased. This is of great importance as SMC^2 schemes are computationally intensive. Combinations of the RBPF with other, simpler, parameter estimation techniques (e.g., [32]) are also possible.

REFERENCES

[1] Y. Aït-Sahalia, *Maximum likelihood estimation of discretely sampled diffusions: a closed-form approximation approach*, Econometrica, **70** (2002), 223–262.

[2] B. D. O. Anderson and J. B. Moore, "Optimal Filtering", Englewood Cliffs, 1979.

[3] C. Andrieu, A. Doucet and R. Holenstein, *Particle Markov chain Monte Carlo methods*, Journal of the Royal Statistical Society Series B-Statistical Methodology, **72** (2010), 269–342.

[4] C. Andrieu, A. Doucet, S. S. Singh and V. B. Tadić, *Particle methods for change detection, system identification and control*, Proceedings of the IEEE, **92** (2004), 423–438.

[5] A. Bain and D. Crisan, "Fundamentals of Stochastic Filtering", Springer, 2008.

[6] A. Beskos, O. Papaspiliopoulos, G. O. Roberts and P. Fearnhead, *Exact an computationally efficient likelihood-based estimation for discretely observed diffusion processes*, J. Roy. Stat. Soc. Ser. B, **68** (2006), 333–382.

[7] G. Buffoni and G. Gilioli, *A lumped parameter model for acarine predator-prey population interactions*, Ecological Modelling, **170** (2003), 155–171.

[8] O. Cappé, S. J. Godsill and E. Moulines, *An overview of existing methods and recent advances in sequential Monte Carlo*, Proceedings of the IEEE, **95** (2007), 899–924.

[9] J. Carpenter, P. Clifford and P. Fearnhead, *Improved particle filter for nonlinear problems*, IEE Proceedings - Radar, Sonar and Navigation, **146** (1999), 2–7.

[10] S. R. Carpenter, K. L. Cottingham and C. A. Stow, *Fitting predator-prey models to time series with observation errors*, Ecology, **75** (1994), 1254–1264.

[11] R. Chen and J. S. Liu, *Mixture Kalman filters*, Journal of the Royal Statistics Society B, **62** (2000), 493–508.

[12] N. Chopin, P. E. Jacob and O. Papaspiliopoulos, *SMC2: an efficient algorithm for sequential analysis of state space models*, Journal of the Royal Statistical Society: Series B (Statistical Methodology), (2012).

[13] J. A. Comiskey, F. Dallmeier and A. Alonso, "Framework for Assessment and Monitoring of Biodiversity", Academic Press, New York, 1999.

[14] R. Douc, O. Cappe and E. Moulines, *Comparison of resampling schemes for particle filtering*, "ISPA 2005: Proceedings of the 4th International Symposium on Image and Signal Processing and Analysis", (2005), 64–69.

[15] A. Doucet, N. de Freitas and N. Gordon (eds.), "Sequential Monte Carlo Methods in Practice", Springer, New York (USA), 2001.

[16] A. Doucet, S. Godsill and C. Andrieu, *On sequential Monte Carlo sampling methods for Bayesian filtering*, Statistics and Computing, **10** (2000), 197–208.

[17] M. Dowd, *A sequential Monte Carlo approach to marine ecological prediction*, Environmetrics, **17** (2006), 435–455.

[18] M. Dowd, *Estimating parameters for a stochastic dynamic marine ecological system*, Environmetrics, **22** (2011), 501–515.

[19] M. Dowd and R. Joy, *Estimating behavioral parameters in animal movement models using a state-augmented particle filter*, Ecology, **92** (2011), 568–575.

[20] G. B. Durham and A. R. Gallant, *Numerical techniques for maximum likelihood estimation of continuous-time diffusion processes*, J. Bus. Econ. Stat., **20** (2002), 297–316.

[21] O. Elerian, S. Chib and N. Shephard, *Likelihood inference for discretely observed nonlinear diffusions*, Econometrica, **69** (2001), 959–993.

[22] B. Eraker, *MCMC analysis of diffusion models with application to finance*, J. Bus. Econ. Stat., **19** (2001), 177–191.

[23] G. Gilioli, S. Pasquali and F. Ruggeri, *Bayesian inference for functional response in a stochastic predator-prey system*, Bulletin of Mathematical Biology, **70** (2008), 358–381.

[24] G. Gilioli, S. Pasquali and F. Ruggeri, *Nonlinear functional response parameter estimation in a stochastic predator-prey model*, Mathematical Biosciences and Engineering, **9** (2012), 75–96.

[25] G. Gilioli and V. Vacante, *Aspetti della dinamica di popolazione del sistema* tetranychus urticae-phytoseiulus persimilis *in pieno campo: implicazioni per le strategie di lotta biologica*, in: Atti del Convegno "La difesa delle colture in agricoltura biologica" - Notiziario sulla protezione delle piante, vol. 13, 2001.

[26] A. Golightly and D. J. Wilkinson, *Bayesian inference for stochastic kinetic models using a diffusion approximations*, Biometrics, **61** (2005), 781–788.

[27] A. Golightly and D. J. Wilkinson, *Bayesian parameter inference for stochastic biochemical network models using particle Markov chain Monte Carlo*, Interface Focus, **1** (2011), 807–820.

[28] N. Gordon, D. Salmond and A. F. M. Smith, *Novel approach to nonlinear and non-Gaussian Bayesian state estimation*, IEE Proceedings-F, **140** (1993), 107–113.

[29] C. Jost and S. P. Ellner, *Testing for predator dependence in predator-prey dynamics: a non-parametric approach*, Proc. Roy. Soc. Lond. B, **267** (2000), 1611–1620.

[30] R. E. Kalman, *A new approach to linear filtering and prediction problems*, Journal of Basic Engineering, **82** (1960), 35–45.

[31] J. Knape and P. de Valpine, *Fitting complex population models by combining particle filters with Markov chain Monte Carlo*, Ecology, **93** (2012), 256–263.

[32] J. Liu and M. West, *Combined parameter and state estimation in simulation-based filtering*, in: A. Doucet, N. de Freitas and N. Gordon (eds.), "Sequential Monte Carlo Methods in Practice", chap. 10, Springer, 2001, pp. 197–223.

[33] J. S. Liu and R. Chen, *Sequential Monte Carlo methods for dynamic systems*, Journal of the American Statistical Association, **93** (1998), 1032–1044.

[34] J. Míguez, D. Crisan and P. M. Djurić, "On the convergence of two sequential Monte Carlo methods for maximum a posteriori sequence estimation and stochastic global optimization", Statistics and Computing

[35] P. D. Moral, "Feynman-Kac Formulae: Genealogical and Interacting Particle Systems with Applications", Springer, 2004.

[36] M. A. Pascual and K. Kareiva, *Predicting the outcome of competition using experimental data: maximum likelihood and Bayesian approaches*, Ecology, **77** (1996), 337–349.

[37] A. R. Pedersen, *A new approach to maximum likelihood estimation for stochastic differential equations based on discrete observations*, Scand. J. Stat., **22** (1995), 55–71.

[38] M. K. Pitt and N. Shephard, *Filtering via simulation: Auxiliary particle filters*, Journal of the American statistical association, **94** (1999), 590–599.

[39] B. L. S. Prakasa Rao, "Statistical Inference for Diffusion Type Processes", Arnold, London, 1999.

[40] C. P. Robert and G. Casella, "Monte Carlo Statistical Methods", Springer, 2004.

[41] K. Shea, H. P. Possingham, W. W. Murdoch and R. Roush, *Active adaptive management in insect pest and weed control: intervention with a plan for learning*, Ecological Applications, **12** (2002), 927–936.

[42] H. Sorensen, *Parametric inference for diffusion processes observed at discrete points in time: a survey*, Int. Stat. Rev., **72** (2004), 337–354.

[43] O. Stramer and J. Yan, *On simulated likelihood of discretely observed diffusion processes and comparison to closed-form approximation*, J. Comput. Graph. Stat., **16** (2007).

[44] J. Y. Xia, R. Rabbinge and W. van der Werf, *Multistage functional responses in a leadybeetle-aphid system: scaling up from the laboratory to the field*, Environmental Entomology, **32** (2003), 151–162.

E-mail address: `lauramartin@ugr.es`
E-mail address: `gianni.gilioli@med.unibs.it`
E-mail address: `ettore.lanzarone@cnr.it`
E-mail address: `joaquin.miguez@uc3m.es`
E-mail address: `sara.pasquali@mi.imati.cnr.it`
E-mail address: `fabrizio.ruggeri@mi.imati.cnr.it`
E-mail address: `druiz@ugr.es`